Stable Growth and Instability of Circumferential Crack in Type 304 Stainless Steel Pipes Under Tensile Load

G. Yagawa, Y. Takahashi
Dept. of Nuclear Engineering, University of Tokyo, 3-1, Hongo 7-chome, Bunkyo-ku, Tokyo 113, Japan

K. Kashima, N. Sasaki
Nuclear Power Engineering Test Center, 2 Akiyama Bldg., 3-6-2, Toranomon, Minato-ku, Tokyo 105, Japan

K. Hasegawa
Mechanical Engineering Research Laboratory, Hitachi Ltd., 3-1-1 Saiwai-cho, Hitachi-shi, Ibaraki-ken 317, Japan

M. Saito
Nuclear Energy Group, Toshiba Corporation, 8, Shinsugita, Isogo-ku, Yokohama-shi, Japan

T. Umemoto
Nuclear Power Division, Ishikawajima-Harima Heavy Industries Co., Ltd., 1-Shin-Nakahara-cho, Isogo-ku, Yokohama 235, Japan

ABSTRACT

The intergranular stress corrosion crackings (IGSCCs) have been found in Type 304 stainless steel piping in some BWR plants. Although there have been no accidents of double-ended pipe fracture resulting from the IGSCCs which might lose the structural integrity of the pipe, it is important to prove for the leak before break (LBB) criterion to be satisfied. The LBB criterion is considered to depend not only on the crack configuration but also on the system compliance, which affects crack stability. In this work, in order to quantitatively study these phenomena, a series of pipe tests and fracture analyses by the finite element method were conducted:

1) Twenty test pipes (6" sch. 80, Type 304 stainless steel) with a surface or through-wall circumferential notch were prepared. Some of the test pipes were quasi-statically tensioned through a high-compliance spring apparatus (10^{-4}mm/N) or directly by 600 ton test rig. The others were loaded dynamically with the same spring apparatus. Applied load, gross elongations, crack opening displacement and crack propagation velocity were measured in each test. In the "quasi-static low-compliance" tests, the cracks have never become unstable during fracture process. On the other hand, the transitions to unstable crack growths have been observed in the "quasi-static as well as dynamic high-compliance" tests. In the latter cases, the crack velocity often reached about 10 to 20 m/sec. Almost entire fracture surfaces of the pipes subjected to dynamic loads through the high-compliance rig have shown characteristics of unstable fracture morphology.

2) In the numerical analyses, a pipe with an initial through-wall crack was studied using two three-dimensional finite element codes developed independently. In the former code, the crack extension was simulated according to the constant crack tip opening angle (CTOA) criterion, while in the latter code, the crack was extended so as to obey the experimental relationship between the crack extension and the gross elongations to obtain the variations of the J-integral and the CTOA as a result. The results by both codes and the experiment were compared regarding the load and the crack opening displacement versus the crack extension. These comparisons have shown good correspondence among them. The stable crack growth amount up to an instability point was predicted using the assumption that the change from stable to unstable fracture may occur at the situation where the total displacement begins to decrease. The present prediction agreed well with the result of the "quasi-static high-compliance" test.

1. Introduction

Circumferential flaws due to the stress corrosion crackings have been found in piping systems of many BWR plants, which became a crucial safety problem of these plants. Although some countermeasures have been successfully employed to reduce the occurrence of these cracks, it is also required to study the safety margin under the presence of such cracks. For the safety assessment of such a flawed structure, the leak before break (LBB) concept has been proposed. Especially, in materials such as Type 304 stainless steel, which is mainly used as the piping material, unstable cleavage fracture can be excluded in the assessment. However, even in these tough materials, there remains a small possibility of unstable ductile fracture, which is largely affected by the system compliance.

With this background, some theoretical and experimental studies on unstable ductile fracture have been performed. Paris et al.[1] proposed the tearing instability criterion based on the J-integral resistance curve, which can account for the influence of the system compliance. Following that, theoretical consideration on the limitation of this approach was made as well as the development of simple estimation methods[2-3]. Besides, in order to verify the criterion experimentally, Paris et al.[4] performed the instability test under the three point bending load. Also, theoretical and experimental investigations for circumferential crack instability were carried out for Type 304 stainless steel pipes subjected to bending load[5-7].

The Leak Before Break Test Group at the Nuclear Power Engineering Test Center in Japan has developed s tensile-type test apparatus with compliance to study the tearing instability behavior of nuclear piping under the quasi-static and dynamic loadings. The crack instability experiments and analyses for cracked specimens were conducted using this machine[8-9]. This paper presents another results of the tearing instability test of circumferentially cracked pipes of Type 304 stainless steel under the quasi-static and dynamic tensile loadings, followed by the theoretical study by the finite element method concerning the experiment.

2. Experiment

2.1 Test Specimens

The austenitic stainless steel (AISI Type 304) pipes of 6 inch and schedule 80 were used for the test specimens. The chemical composition and the mechanical properties are shown in Tables 1 and 2, respectively. Pipe geometry and initial notch configuration are shown in Fig. 1. Twenty pipes with an inner-surface or through-wall notch in the circumferential direction were prepared. Notch geometries and test conditions are summarized in Table 3.

The initial notches with width of 0.3 mm were introduced by electro-discharge machining in the heat-affected zone (HAZ) of three welded pipes (Specimen No. CPW-1, CPW-3H and CPW-2) or in the plain base metal of the as-received ones. The maximum depth of inner-surface notch denoted by c in Fig.1 is 0.3t or 0.7t (t : pipe thickness).

2.2 Test Condition and Measurement

As shown in Table 3, three types of experiments are carried out in order to study the influence of compliance and dynamic effect on fracture behavior. The first is the "quasi-static low-compliance" test in which a normal low-compliance testing apparatus is used. The second is the "quasi-static high-compliance" test using the high-compliance apparatus

shown in Fig. 2, in which the test pipes are quasi-statically loaded through a spring with compliance of 10^{-4}mm/N. Finally, in the third type of the experiment, six pipes are loaded dynamically with the test device with compliance (the "dynamic high-compliance" test). These tests are conducted at room temperature or 285°C in air.

Applied load, gross elongations (gauge length : 250 mm) and crack opening displacement are continuously recorded in the tests. Stable crack growth is measured by observing the pipe surface in the low-compliance test. Since unstable crack extension is expected in the high-compliance tests, crack gauges are attached on the pipe surface to measure crack propagation velocity from their break time.

2.3 Test Results

Maximum loads for all the specimens are summarized in Table 3. The fracture behaviors of the specimens were dependent on the test types. Typical schematic drawings of the fracture surfaces for the three test types are shown in Fig. 3.

In the "quasi-static low-compliance" tests, cracks never became unstable and fracture surfaces were flat in the entire regions. In the "quasi-static high-compliance" tests, both ductile flat and 45° shear parts were observed in the fracture surfaces. After stable ductile flat cracks of 50 to 70 mm length, the pipes exhibited a rapid double ended fracture. The reductions of wall thickness in the stable flat cracked area were about 50 % and those in the unstable shear cracked area were 25 %. In the case of the "dynamic high-compliance" tests, negligible or very small flat cracked surface was observed and almost all of the fracture surface was of shear fracture type.

The lengths of stable growth of ductile flat crack for as-received and welded through-notched specimens are summarized in Fig. 4, which involves the "quasi-static low-compliance" test, the "quasi-static high-compliance" test and the "dynamic high-compliance" test denoted respectively as St., Cm. and Dy.. It can be seen from the figure that the difference between the as-received and the welded specimens is negligible.

Figure 5 shows the variation of crack propagation velocity in two pipes subjected to the "quasi-static high-compliance" loading which contain through wall initial notches of 30 and 120 degrees, respectively. In this figure, Ch.1 and Ch.2 correspond to one and the other sides of crack propagation, respectively. Crack propagation velocities are seen to increase rapidly with crack extension until about 10 m/sec.

3. Theoretical Consideration and Discussion

Crack extension analysis under the elastic-plastic condition is needed in order to estimate the strength of cracked pipes, for which the finite element method is expected to be an effective tool. Regarding this, two three-dimensional elastic-plastic finite element codes named PIPE-6 and PIPE-16 have been developed for the purpose of the crack extension analysis in pipes. Here, we perform numerical analysis on the crack extension for the pipe using these codes and discuss the fracture behavior of circumferentially cracked pipes tested.

3.1 Models for Numerical Analysis

Geometry and Boundary Condition Taken as an object of calculation is the "quasi-static high-compliance" test specimen with a through-wall initial notch of 30 degrees. Figure 6 shows the finite element model for the calculation. To economize the computer cost, we model only the 1/12 part of the test pipe, where the gross elongations between points A and

C and between A' and C' are measured. Linearly interpolated along the circumferential direction, these elongation data are used to prescribe the displacement at the end of the finite element model. The 6-noded and 16-noded isoparametric elements are used in PIPE-6 and PIPE-16, respectively. The finite element subdivisions for the both codes are shown in Figs. 6(b) and 6(c).

Material Properties From the uniaxial tension test, the Young's modulus and the yield stress are determined to be 185.1 GPa and 234 MPa, respectively. The Poisson's ratio is assumed to be 0.3. A bilinear approximation of the equivalent stress - equivalent plastic strain relation is used for the plastic flow property.

3.2 Methods for Numerical Analysis

Table 4 describes the characteristics of the numerical method employed in both codes. As can be seen in the table, the J-integral is calculated based on the virtual crack extension technique[10] with PIPE-16.

As a criterion for crack extension, the experimental relation between the gross elongations measured along the lines AB and A'B' shown in Fig. 6 and the crack extension amount is utilized in PIPE-16 (Generation phase simulation). In PIPE-6, on the other hand, the constant CTOA criterion is assumed and the critical CTOA of 0.2 radian, which is obtained from the analysis for center cracked plates[11], is employed (Application phase simulation). In both calculations, the value of CTOA is evaluated from the crack opening displacement at the corner node nearest to the crack tip. The crack extension is realized by the nodal releasing technique in both codes, in which the nodal reaction force is eliminated in several increments after the removal of nodal restraint.

3.3 Numerical Results

Load and Deformation Characteristics Figure 7 shows the variations of the applied load and the crack opening displacement COD at the point 10 mm apart from the initial notch tip with the crack extension Δa. The applied load first reaches the maximum value and then decreases gradually with the stable crack growth. This maximum load is calculated to be 1303 kN (PIPE-16) or 1392 kN (PIPE-6), while the value of 1274 kN is obtained in the experiment. The values of COD, increasing almost linearly with the crack extension, are shown in the figure with the experimental values.

Resistance Curves based on J-integral and CTOA Approaches Crack tip parameters such as the J-integral and the crack tip opening angle (CTOA) are obtained from the numerical solutions by PIPE-16, the code for generation phase simulation. The J-integral value, being about 1 MN/m at the crack initiation, increases remarkably with the stable crack growth as shown in Fig. 8. These characteristics in the J-resistance value for the pipe specimen are nearly the same as those of the center cracked plate specimens[11] plotted in the figure. Figure 9 shows the CTOA resistance curve calculated using PIPE-16. As shown in the figure, the CTOA obtained by the present analysis is relatively close to the CTOA band calculated for the center cracked plate specimens[11].

From these results, the J-integral and CTOA approaches are considered to be effective criteria which can describe the crack initiation and stable crack extension, independent of the configuration of cracked specimens.

Crack Instability Instability point of the circumferential crack in the pipe specimen is predicted from the condition that the total displacement remains constant during the

crack extension. The total displacement Vt is represented as the sum of the displacement of the pipe specimen Vs and that of the spring for high compliance itself Vc. Assuming the pipe displacement Vs to be equal to the COD and using the relation $Vc=C \cdot P$ with P being the load and C being the compliance, the total displacement $Vt(=Vs+Vc)$ is obtained as a function of the crack extension amount Δa.

Figure 10 shows the variations of Vt, Vs and Vc with the crack extension obtained using the codes PIPE-6 and PIPE-16, respectively. Employing the instability condition of $dVt/da=0$, the stable crack extension amount up to the instability Δa_{inst} is predicted to be 48.9 and 51.3 mm by PIPE-6 and PIPE-16, respectively. Experimental measurement on the fracture surface has shown that the unstable crack propagation begins after the stable crack extension of 50 to 60 mm. Thus, the finite element solutions seem to predict the crack instability point with comparably good agreement with the experimental result, although the theories give somewhat shorter stable crack extensions than the experiment.

4. Conclusions

The fracture behaviors of Type 304 stainless steel pipes with a circumferential crack were studied with the experiment and the finite element analysis. The following results are obtained:

1) In the "quasi-static low-compliance" test, cracks extend stably throughout showing the flat fracture surfaces. The changes from stable to unstable crack extension, which is characterized by the 45° shear fracture surfaces, are observed in the "quasi-static high-compliance" test as well as the "dynamic high-compliance" test.

2) Maximum crack velocity in the unstable fracture region exceeds 10 m/sec.

3) From the application and generation phase simulations by the finite element methods, it is found that the J-integral and the CTOA are effective parameters for the crack initiation and the stable crack extension.

4) Crack instability is predicted from the stationary condition of the controlled displacement, taking the effect of the compliance in the loading system into account.

References

(1) Paris, P. C., Tada, H., Zahoor, A., and Ernst, H., "The Theory of Instability of the Tearing Mode of Elastic-Plastic Crack Growth", Elastic-Plastic Fracture, ASTM STP 668, 1979, pp.5-36.

(2) Hutchinson, J. W. and Paris, P. C., "Stability Analysis of J-controlled Crack Growth", Elastic-Plastic Fracture, ASTM STP 668, 1979, pp.37-64.

(3) German, M. D. and Kumar, V., "Elastic-Plastic Analysis of Crack Opening, Stable Growth and Instability Behavior in Flawed 304SS Piping", Aspects of Fracture Mechanics in Pressure Vessels and Piping, ASME PVP, Vol.58, 1982, pp.109-141.

(4) Paris, P. C., Tada, H., Zahoor, A. and Ernst, G., "An Initial Experimental Investigation of Tearing Instability Theory", Elastic-Plastic Fracture, ASTM STP 668, 1979, pp.251-265.

(5) Tada, H., Paris, P. C. and Gamble, M., "A Stability Analysis of Circumferential Cracks for Reactor Piping Systems", Fracture Mechanics: Twelfth Conference, ASTM STP 700, pp.296-313.

(6) Zahoor, A. and Kanninen, M. F., "A Plastic Fracture Mechanics Prediction of Fracture Instability in a Circumferentially Cracked Pipe in Bending - Part I : J-integral

Analysis", Journal of Pressure Vessel Technology, Trans. ASME, Ser. J, Vol. 103, 1981, pp.352-358.

(7) Wilkowski, G. M., Zahoor, A. and Kanninen, M. F., "A Plastic Fracture Mechanics Prediction of Fracture Instability in a Circumferentially Cracked Pipe in Bending - Part II : Experimental Verification on a Type 304 Stainless Steel Pipe", Journal of Pressure Vessel Technology, Trans. ASME, Ser. J, Vol. 103, 1981, pp.359-365.

(8) Yagawa, G., Takahashi, Y. and Ando, Y., "Theoretical and Experimental Study on Unstable Fracture for Type 304 Stainless Steel Plates with a Soft Tensile Testing Machine", Engineering Fracture Mechanics, Vol. 16, No. 5, 1982, pp.721-731.

(9) Yagawa, G., Kashima, K., Kato, N., Saito, M., Hasegawa, K. and Umemoto, T., "Fracture Behaviors of Type 304 Stainless Steel Pipes with Circumferential Inner-surface Crack under Cyclic Tension and BWR Emvironment", to be presented at ASME PVP Conference, Portland, Oregon, 1983.

(10) Parks, D. M., " Virtual Crack Extension : a General Finite Element Technique for J-integral Evaluation", Proceedings of the First International Conference on Numerical Methods in Fracture Mechanics, (edited by Luxmoore, A. R. and Owen, D. R. J.), Swansea, 1978, pp.464-478.

(11) Takahashi, Y. and Yagawa, G., "Study on Unstable Ductile Fracture of Nuclear Primary Piping, Second Report: Finite Element Analysis of Resistance Curves and Stability Analysis Using Simplified Method", Proceedings of the Japan Society of Mechanical Engineers, No. 820-12, 1982, pp.142-149. (in Japanese).

Table 1 Chemical Composition

(wt %)

	C	Si	Mn	P	S	Ni	Cr
JIS Spec.*	≦0.08	≦1.00	≦2.00	≦0.040	≦0.030	8.00-11.00	18.00-20.00
Present	0.05	0.50	1.51	0.026	0.003	9.30	18.30

* Japanese Industrial Standard Specification

Table 2 Mechanical Properties

	Room Temperature			285°C		
	0.2% Proof Strength MPa	Tensile Strength MPa	Elongation %	0.2% Proof Strength MPa	Tensile Strength MPa	Elongation %
JIS Spec.	≧206	≧520	≧35	-	-	-
Present	284	588	67	167	431	38

Table 3 Test Conditions and Maximum Load

Test type	Specimen number(1)	Notch geometry(3)		Maximum load(kN)
		2α(deg)	c/t(2)	
Static low-compliance test	CP-1	30	1	1176
	CP-2	60	1	1039
	CP-3	90	1	909
	CP-12	60	0.7	1044
Static high-compliance test	CP-4	30	1	1278
	CP-5	60	1	1084
	CP-6	90	1	977
	CP-7	120	1	852
	CPW-1	60	1	1004
	CP-9H	60	1	725
	CP-10	60	0.7	1071
	CP-11	60	0.3	——
	CP-14H	60	0.7	840
	CPW-3H	60	1	753
Dynamic high-compliance test	CP-8	60	1	1115
	CPW-2	60	1	1107
	CP-13H	60	1	765
	CP-15	90	1	959
	CP-16	60	0.7	1143
	CP-17	60	0.3	1656

Note: (1) W indicates welded specimen.
H indicates high temperature test(285°C).
(2) c/t = 1 means through-wall notch.
(3) See Fig. 1.

Table 4 Methods for Solutions

Computer code	PIPE-6	PIPE-16
Element type	6-noded isoparametric	16-noded isoparametric
Number of nodes	330	456
Number of elements	280	63
Plasticity theory	Flow theory (Isoparametric hardening)	
Geometrical nonlinearity	Small strain	
Calculation scheme	Tangent modulus (Partial stiffness)	
Strain hardening property	Bilinear approximation	
J-integral calculation	——	Virtual crack extension method
Crack extension technique	Nodal releasing	
Crack extension criterion	Crack tip opening angle (CTOA)	Gauge displacements
Simulation technique for crack extension	Application phase	Generation phase

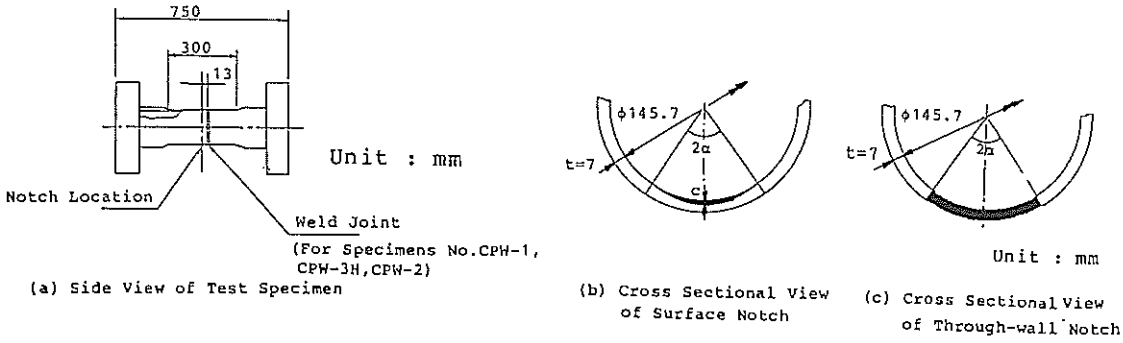

Fig.1 Geometry of Test Pipe and Notch

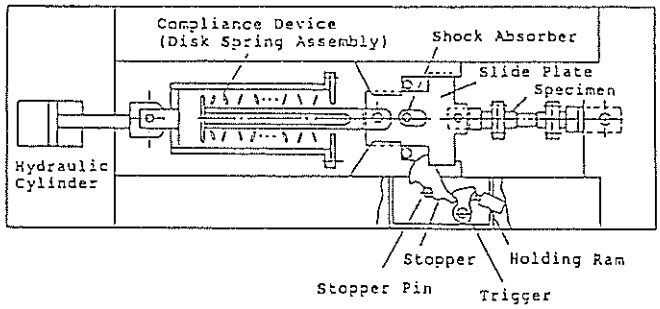

Fig.2 Testing Apparatus

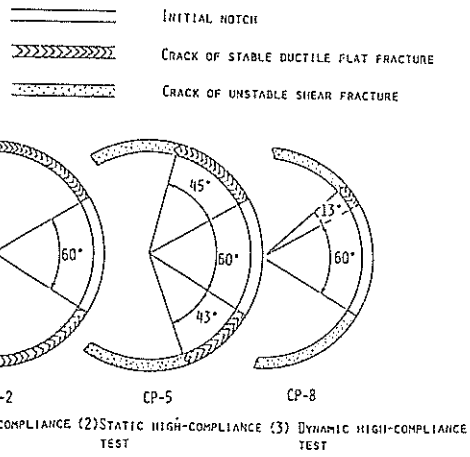

Fig.3 Cross-sectional View of Post-fracture Surface

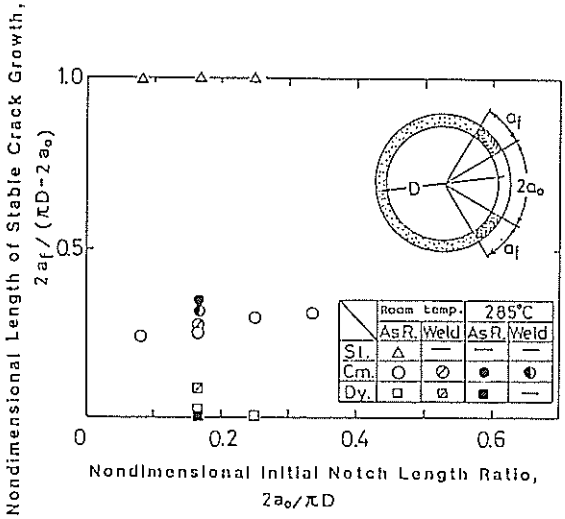

Fig.4 Nondimensional Length of Stable Crack Growth vs. Nondimentional Initial Notch Length

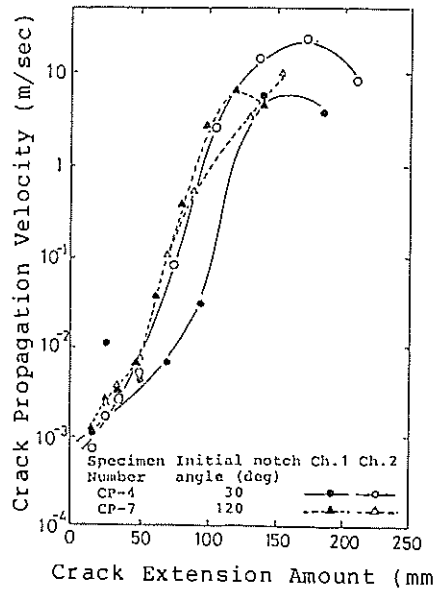

Fig.5 Crack Propagation Velocity vs. Crack Extension Amount for Specimens No. CP-4 and CP-7

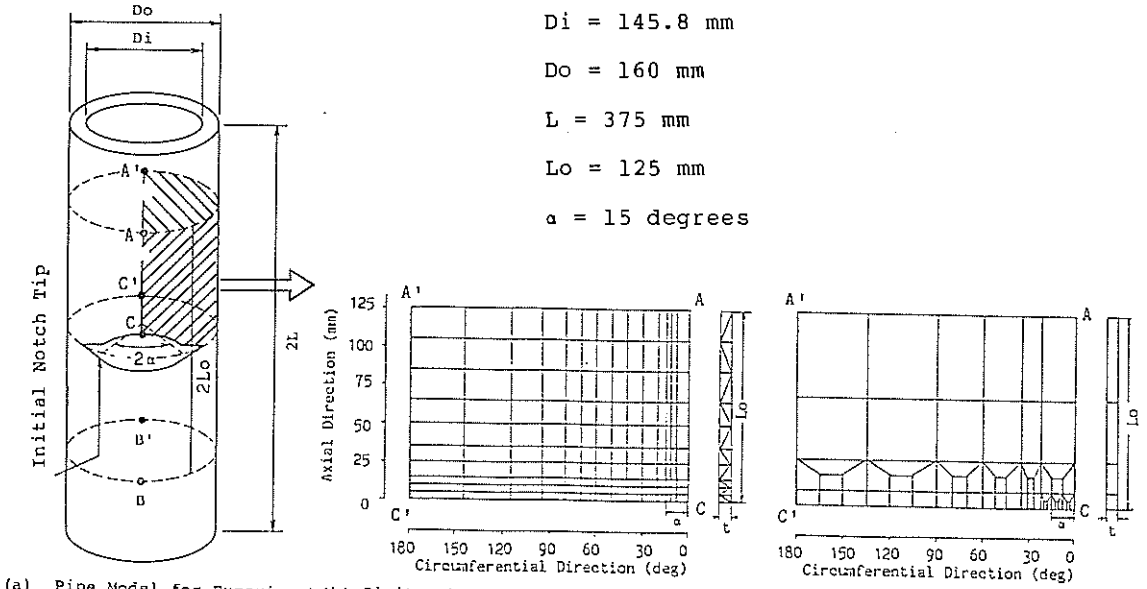

(a) Pipe Model for Experiment (b) Finite Element Subdivision for PIPE-6 (c) Finite Element Subdivision for PIPE-16

Fig.6 Finite Element Model for Cracked Pipe

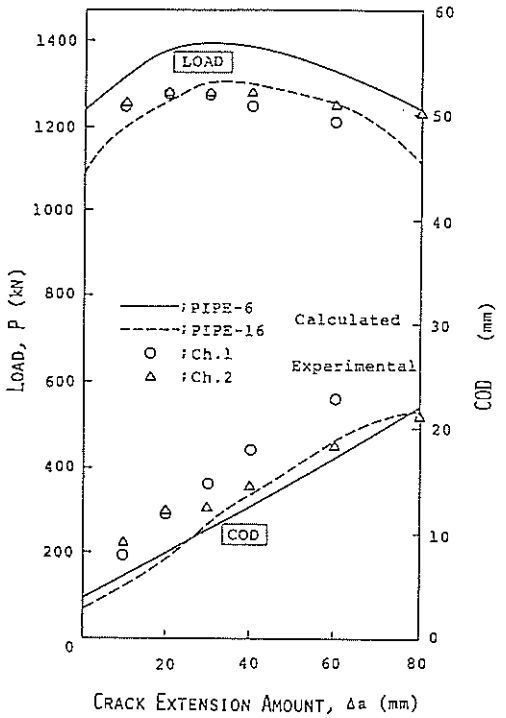

Fig.7 Variations of Load and Crack Opening Displacement with Crack Extension (Specimen No. CP-4)

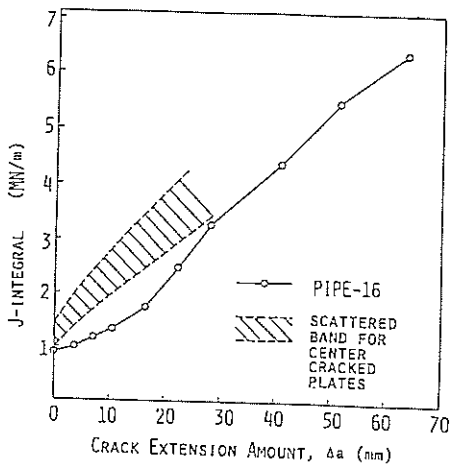

Fig.8 J-integral vs. Crack Extension Amount

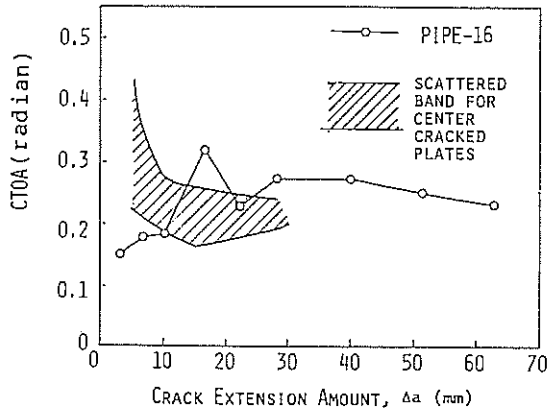

Fig.9 CTOA vs. Crack Extension Amount

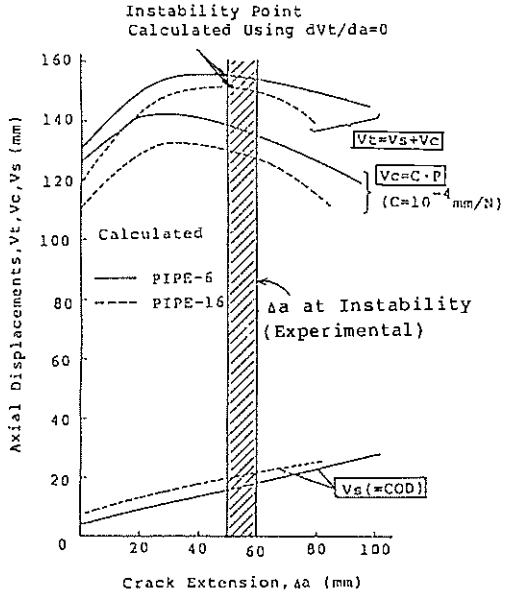

Fig.10 Prediction of Tearing Instability
(Specimen No. CP-4)